An accurate pose measurement method of workpiece based on rapid extraction of local feature points*

ZHANG Jiangtao[1,2], QIAO Zhifeng[1,2], and WANG Shihao[1,2]**

1. *Tianjin Key Laboratory for Advanced Mechatronic System Design and Intelligent Control, School of Mechanical Engineering, Tianjin University of Technology, Tianjin 300384, China*
2. *National Demonstration Center for Experimental Mechanical and Electrical Engineering Education, Tianjin University of Technology, Tianjin 300384, China*

(Received 25 September 2021; Revised 22 October 2021)

Ceramic sanitary products with complex curved surfaces are generally fragile and difficult to clamp. If the industrial robot is utilized to realize the automatic grinding of such products, the precise positioning of the product is required firstly. In this paper, an accurate pose measurement system for complex curved surface parts is designed by point cloud registration algorithm. In order to improve the stability of the system, this paper combines the advantages of normal vector features and fast point feature histogram (*FPFH*) features, and proposes a point cloud registration algorithm based on the rapid extraction of local feature points. Experimental results verify that the improved algorithm has improved both efficiency and accuracy, and the system can effectively achieve accurate positioning of products.

Document code: A **Article ID:** 1673-1905(2022)06-0372-6

DOI https://doi.org/10.1007/s11801-022-1152-4

In the manual grinding process of complex curved surface parts represented by ceramic sanitary products, there generally exist such problems, such as poor uniformity, serious dust pollution, low production efficiency and high production cost. The automatic grinding[1] by robots can liberate the workforce, improve the accuracy and consistency of products, and ameliorate the labor environment of workers. Because the product has vulnerable surface without obvious point and line features, if the industrial robot is utilized to realize the automatic grinding of such products, the positioning of workpieces has become the primary problem to be solved. The point cloud registration algorithm can unify two point clouds in one coordinate system, and we can gain their position transition matrix. This paper will study the accurate pose measurement method for complex curved surface based on point cloud registration algorithm in detail.

Point cloud registration is widely used in various occasions. KONG[2] identifies geomorphological changes of coastal cliffs through point cloud registration. SHU et al[3] applied point cloud registration algorithm to flatness measurement. GUO et al[4] studied the registration of large karst caves with different scanning methods. TSAI et al[5] carried out indoor scene registration based on red green blue and depth (RGB-D) camera calibration.

Registration accuracy and registration efficiency are the important indicators of point cloud registration algorithm and the important reference points of registration effects. MOHAMMAD et al[6] applied Nelder-Mead and gravitational search algorithm in point clouds registration process. SHI et al[7] improved iterative closest points (ICP) algorithm based on *k*-dimensional (KD)-tree, which greatly improved the search efficiency. SUN et al[8] designed an automatic three-dimensional (3D) point cloud registration method based on regional curvature maps. ZHANG et al[9] improved the point cloud registration algorithm by differential evolution algorithm. LI et al[10] improved point cloud registration algorithm based on normal vector angle. RAN et al[11] improved the accuracy of point cloud registration algorithm based on scale invariant feature transform (SIFT). REN et al[12] proposed a color point cloud registration algorithm based on hue, which has good robustness at different lighting conditions.

On the basis of the above research, this paper will build a complete and accurate 3D data measurement system for complex curved surface products, and analyze the accuracy reliability of this system. Firstly, the 3D point cloud data of products is scanned through lidar. Secondly, the accuracy of whole measurement system is analyzed based on the ranging accuracy of lidar and the rotating accuracy of turntable, and the results could effectively guide the design and type-selection of such 3D measurement system. In addition, in consideration of the

* This work has been supported by the Tianjin Key Research and Development Project (No.19YFSLQY00050), the Tianjin Science and Technology Major Project and Engineering Project (No.19ZXZNGX00100), and the Tianjin Enterprise Science and Technology Commissioner Project (No.20YDTPJC00790).
** E-mail: qiaozhifeng@163.com

dependency of the traditional ICP algorithm on good initial position, this paper combines the advantages of normal vector features and fast point feature histogram features, and proposes a point cloud registration algorithm based on the rapid extraction of local feature points. Finally, this paper carries out a registration experiment in order to verify the effectiveness of the complete system scheme and the related improved algorithm. The experimental results show that this system has simple structure, and the improved algorithm has improved both efficiency and accuracy. The measurement system designed in this article could achieve the accurate positioning of products and provide the research basis for the automatic grinding of complex curved surface parts.

As shown in Fig.1, the data acquisition device mainly has four components, which are two-dimensional (2D) lidar, turntable, servo controller, computer and related mechanical components. Compared with 3D lidar in the market, 2D lidar has the features of smaller volume, lower price, higher scanning speed, and high accuracy, which is conveniently installed on various indoor and outdoor places. The computer sends commands to the lidar and the controller at the same time to ensure that while the lidar scans, the turntable controlled by the servo controller starts to rotate. After the data acquisition is completed, the lidar sends the data to the computer.

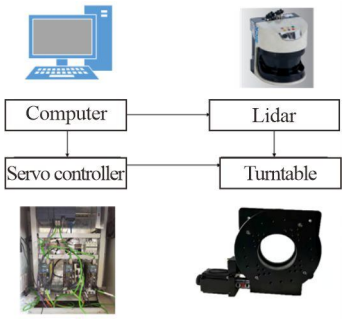

Fig.1 Schematic of the data acquisition system

As shown in Fig.2, $\{L\}$ is the lidar coordinate system and $\{C\}$ is the turntable coordinate system. The rigid body transformation between lidar and turntable can be expressed as

$$\boldsymbol{T}_{CL} = (t_x, t_y, t_z, \phi, \varphi, \gamma), \tag{1}$$

where $\boldsymbol{T}_{CL}$ refers to the matrix for coordinate transformation between $\{C\}$ and $\{L\}$, t_x, t_y and t_z refer to the amount of translation in x, y and z directions, respectively, and ϕ, φ and γ refer to the amount of rotation in x, y and z directions, respectively.

Since the data points measured by lidar are based on their own coordinate system, it is necessary to transform these points to the turntable coordinate system through the above transformation. In the process of data acquisition by lidar, the angle rotated by the turntable between each frame of data is θ. While the lidar collects a frame of data, the turntable rotates θ, and a new coordinate system will be generated accordingly. The points under each new coordinate system are converted to $\{C\}$ (i.e., the coordinate system generated when the lidar collects the first frame of data) through the rotation transformation. For example, the nth frame of data needs to rotate $(n-1)\cdot\theta$ around the z axis. All the collected data points can be unified to the same coordinate system, so as to realize the transformation from 2D data to 3D data.

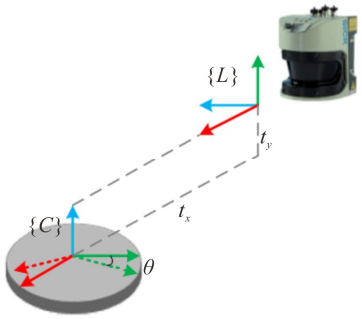

Fig.2 Coordinate transformation diagram

All the 3D points after coordinate transformation can be visualized. Due to the influence of experimental environment, there are a large number of outliers in the transformed 3D data, so point cloud filtering must be performed. The common methods of point cloud filtering include direct pass filtering, voxel filtering, statistical filtering, conditional filtering and radius filtering. Since the noise points of the data in this paper have obvious deviation in position, conditional filtering is selected for denoising. Fig.3(a) and (b) are the point cloud models before and after filtering, respectively.

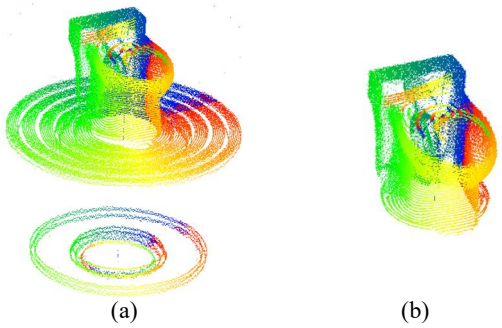

Fig.3 (a) Model diagram of point cloud before filtering; (b) Model diagram of point cloud after filtering

According to the above processing, it is found from the analysis of the whole measurement process that the main errors come from two aspects, namely the ranging accuracy error of lidar, and the rotation accuracy error of turntable.

As shown in Fig.4, the rotation error of the turntable is $\pm e_a$. The horizontal distance from the center point of the lidar to the center point of the turntable is d, and the height distance is h. The maximum angle when the lidar scans is β, and the ranging accuracy error of the lidar is

$\pm e_L$. Affected by the above two errors, the variation range of the error value of point $\boldsymbol{P}$ is shown in the orange hook face in Fig.4. Assume that the distance from the center point of the lidar to the point $\boldsymbol{P}$ is L.

In consideration of the impact of the accuracy error factors of turntable and scanner, the maximum error $e_{\max}$ can be calculated as

$$e_{max}=(d^2+[d-(L+e_L)\cos\beta]^2-2d\cos\alpha[d-(L+e_L)\cos\beta]+[(L+e_L)\sin\beta]^2)^{\frac{1}{2}}-L, \quad (2)$$

where d=2, h=2.38, e_α=0.01, e_L=0.01, and β=45°.

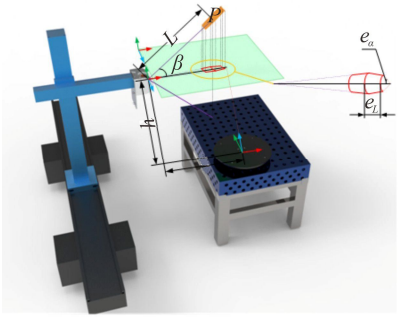

Fig.4 Diagram of system accuracy analysis

Fig.5 shows the trend diagram of the maximum error $e_{\max}$ with the change of L. It can be seen that when L is 1.38 m, the maximum error value is the smallest, which is 0.042 mm. For the actual scanning scenarios, if the model of lidar and turntable are selected, when the product is placed about 0.98 m away from the lidar, the effect of scanning is the best.

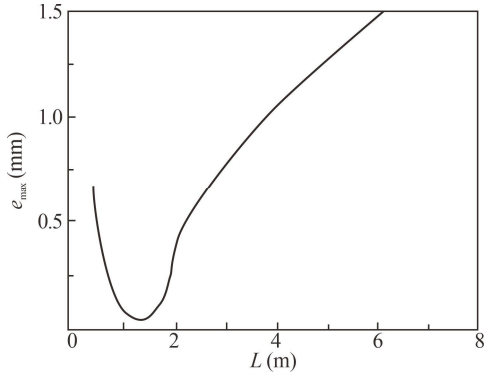

Fig.5 The maximum error e_{max} as a function of L

The point cloud registration algorithm includes rough registration and precise registration, and the algorithm takes a long time. Moreover, the ICP registration algorithm relies on the initial position of the point cloud, which is easy to fall into the local optimal solution, so the accuracy of the algorithm can't be stable. Therefore, this paper proposes a point cloud registration algorithm for the industrial field with short time consuming and stable accuracy.

Because the data points scanned by lidar are huge, this paper extracts the feature points of each point cloud based on the normal vector in order to improve the speed of point cloud registration. Observation shows that in the flat area of the point cloud, the normal vector is densely distributed and the degree of change is small. In the uneven area of the point cloud, the normal vector changes greatly. Therefore, this paper selects feature points located in uneven areas.

Assuming that there is $\boldsymbol{P}_i$ in the original point cloud, the points inside the neighborhood k are P_{i1}, P_{i2}, …, P_{ik}.

$$\bar{P}_i=\frac{1}{k}\sum_{j=1}^{k}P_{ij}, \quad (3)$$

$$\boldsymbol{M}=\frac{1}{k}\sum_{i=1}^{n}(P_{ij}-\bar{P}_i)(P_{ij}-\bar{P}_i)^{\mathrm{T}}, \quad (4)$$

where $\bar{P}$ refers to the centroid of neighborhood, $\boldsymbol{M}$ is the covariance matrix of $\boldsymbol{P}_i$, the eigenvector corresponding to the minimum eigenvalue of $\boldsymbol{M}$ is used as the normal vector of $\boldsymbol{P}_i$.

The points whose absolute value of the inner product of the normal vector is less than ε_1 are selected as feature points.

For the point clouds $\boldsymbol{P}$ and $\boldsymbol{Q}$ to be registered, the above method is used to extract feature points effectively, and then the set P_m and Q_n of feature points are obtained respectively, where m and n are the numbers of points of $\boldsymbol{P}$ and $\boldsymbol{Q}$.

There is no topological structure between the obtained point clouds, so the extracted feature points should be characterized. In view of this, fast point feature histogram (*FPFH*) is used to estimate the normal feature, and the histogram is constructed using the information of the normal vector and the surface curvature feature of the neighborhood. This paper calculates the angle of the normal vector between the registration point and k quantity points in the neighborhood, and then obtains a multi-dimensional histogram. The calculation steps are as follows.

As shown in Fig.6, for each query point $\boldsymbol{P}_q$, this paper defines a local coordinate system and calculates the relative position deviation of the normal vectors $\boldsymbol{n}_q$ and $\boldsymbol{n}_k$ of $\boldsymbol{P}_q$ and $\boldsymbol{P}_k$, called the simplified point feature histogram (*SPFH*). The neighborhood points of $\boldsymbol{P}_q$ are shown in the shaded part of Fig.7.

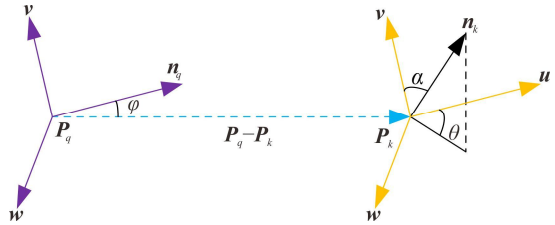

Fig.6 Local coordinate system

The calculation formula of relative position deviation is as follows

$$\alpha=\boldsymbol{v}\cdot\boldsymbol{n}_q,$$

$$\varphi=\boldsymbol{u}\cdot\frac{\boldsymbol{P}_q-\boldsymbol{P}_k}{d},$$

$$\theta = \arctan(\boldsymbol{w} \bullet \boldsymbol{n}_q, \boldsymbol{u} \bullet \boldsymbol{n}_k), \tag{5}$$

where d is the Euclidean distance between two points. We calculate the triplet (α, φ, θ) between query points and neighborhood points in the whole region and count them into 11 subintervals. Then we can obtain the 33-dimensional histogram vector, called *SPFH*.

The weighted *FPFH* can be calculated by

$$FPFH(\boldsymbol{P}_q) = SPFH(\boldsymbol{P}_q) + \frac{1}{k}\sum_{i=1}^{k}\frac{1}{w_i} \cdot SPFH(\boldsymbol{P}_q), \tag{6}$$

where w_i represents the distance weight between $\boldsymbol{P}_q$ and the ith neighborhood point.

The feature vector point sets $\boldsymbol{P}'$ and $\boldsymbol{Q}'$ can be obtained through the above steps.

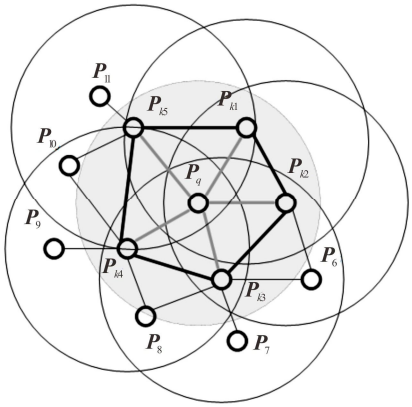

Fig.7 Influence range diagram of the *K* neighborhood centered on P_q of *FPFH*

In the above steps, feature descriptors are calculated for each feature point, and we can find the correct matching point in $\boldsymbol{Q}'$ for each point of $\boldsymbol{P}'$. Firstly, we select an appropriate threshold ε_2. Secondly, the bidirectional nearest neighbor distance ratio criterion is adopted to remove the matching point pairs whose distance between feature descriptors is greater than ε_2, and the remaining matching point pairs are reserved as initial matching point pairs. In the end, the initial transformation matrix is calculated by the unit quaternion method.

After the rough registration, target point cloud has acquired a better initial position. ICP algorithm is used in this paper for precise registration, which calculates the motion parameters according to the geometric features between source point cloud and target point cloud. Then these parameters are used to transform the points, so we can get new target point cloud and the source point cloud. The above process is repeated by continuing to determine new correspondence between the registration point clouds in order to minimize the objective function. The objective function is as follows

$$f(\boldsymbol{R}, \boldsymbol{T}) = \frac{1}{n}\sum_{i=1}^{n}\left\|\boldsymbol{P}_i - \boldsymbol{R} \cdot \boldsymbol{Q}_i - \boldsymbol{T}\right\|^2, \tag{7}$$

where $\boldsymbol{R}$ and $\boldsymbol{T}$ represent rotation and shift parameters respectively, and $\boldsymbol{P}_i$ and $\boldsymbol{Q}_i$ represent source point cloud and target point cloud, respectively.

In order to verify the effectiveness of the improved algorithm, this paper conducts registration experiments of different algorithms. In this experiment, Visual Studio 2015 is used as the software development platform, C++ is used as the programming language and point cloud data is acquired based on point cloud library.

Fig.8 shows the diagram of experimental device during data acquisition process. Based on this environment, the point cloud data of ceramic embryo is obtained.

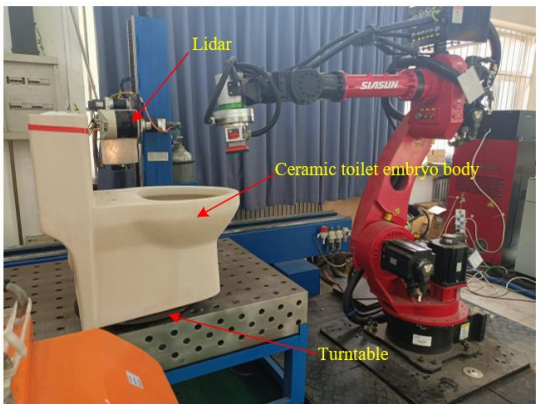

Fig.8 Diagram of the experimental setup

In this paper, 3D standard design model is used as the source point cloud and the point cloud model after experimental acquisition is used as the target point cloud. 3D shape context (3DSC), normal distribution transformation (NDT), four-point consistent set (4PCS) and the improved algorithm in this paper are respectively used for registration experiments. There are 47 832 data points in this experiment, and the accuracy of different algorithms can be compared by calculating the root mean square error (*RMSE*). The calculation formula is shown as follows

$$RMSE = [\frac{1}{N_{\mathrm{p}}}\sum_{i=1}^{n}(\boldsymbol{R}\boldsymbol{p}_i + \boldsymbol{T} - \boldsymbol{q}_i)^2]^{\frac{1}{2}}, \tag{8}$$

where N_{p} refers to the number of source point clouds, $\boldsymbol{p}_i$ refers to the point in the source point cloud, and $\boldsymbol{q}_i$ refers to the point set of the corresponding $\boldsymbol{p}_i$ in the target point cloud.

At the same time, the time required for each registration method to complete registration is recorded in the experiment. As shown in Tab.1, the improved algorithm in this paper has better performance in time and error compared with other algorithms. Because 3DSC needs to calculate the surface shape characteristics of point cloud, which increases the amount of calculation. The reason for 4PCS is that it is necessary to search the common four-point basis of the whole point cloud, which is of high computational complexity and time-consuming. NDT has the largest error, but its efficiency is at a medium level. The improved algorithm in this paper screens feature point pairs based on normal vector features and *FPFH* features, which effectively reduces the amount of calculation.

Tab.1 Registration time and error comparison

Registration algorithm	Time (s)	*RMSE* (mm)
3DSC	168.526	18.362
NDT	67.917	40.648
4PCS	346.472	27.513
Improved algorithm in this paper	6.435	8.667

Since the point clouds of registration are on the same horizontal plane, the translation distance errors of the registration point cloud relative to the target point cloud on the x and y axes and the rotation angle error of the z axis are recorded in the experiment. As can be seen from Tab.2, the translation distance error on the x-axis is in descending order of NDT, 3DSC, 4PCS, and the algorithm is improved in this paper. On the y-axis, the translation distance error in descending order is NDT, 4PCS, 3DSC, and the algorithm is improved in this paper. The rotation angle error on the z-axis is in descending order of NDT, 4PCS, 3DSC, and the algorithm is improved in this paper. As can be seen from Fig.9, NDT has the worst registration effect as a whole. The improved algorithm in this paper performs well in the overall effect, and the registration accuracy can meet the industrial requirements.

Tab.2 Errors of the point cloud on the *X*, *Y* and *Z* axes

Registration algorithm	x-axis distance error (mm)	y-axis distance error (mm)	z-axis rotation error (°)
3DSC	0.217 5	0.104 9	0.317 1
NDT	0.176 1	0.247 3	1.472 8
4PCS	0.018 5	0.156 4	0.831 6
Improved algorithm in this paper	0.003 4	0.007 1	0.031 4

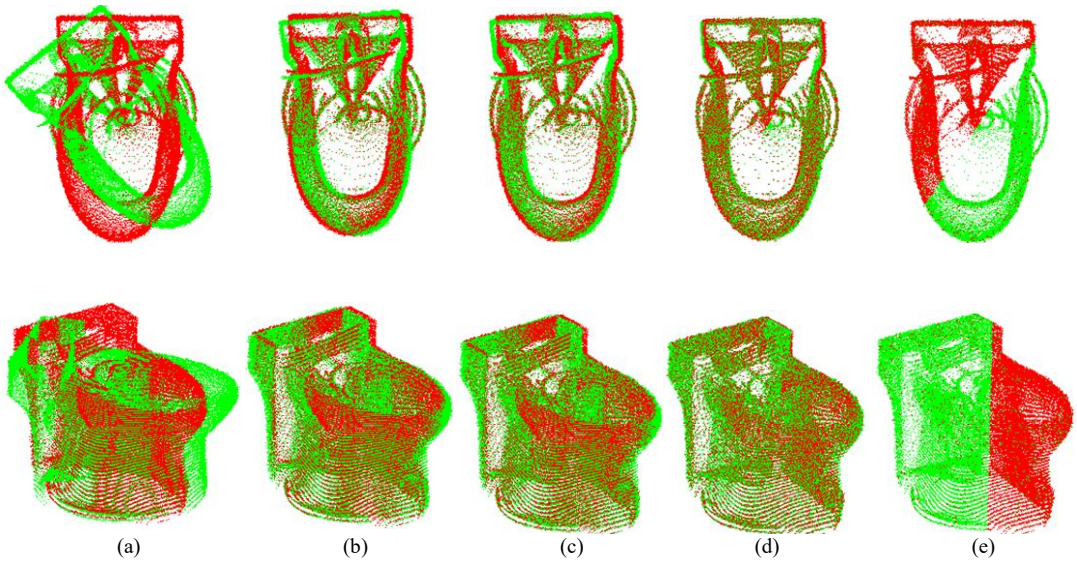

Fig.9 Registration effects of point cloud using different algorithms: (a) Initial position of point cloud; (b) NDT; (c) 4PCS; (d) 3DSC; (e) Improved algorithm in this paper

Aiming at the positioning problem of workpieces with complex curved surface features represented by ceramic sanitary wares in the industrial field, an accurate pose measurement method based on rapid extraction of local feature points is proposed in this paper. Firstly, a data acquisition system is built based on lidar and turntable. Secondly, the accuracy of the whole measurement system is analyzed, and the analysis results could effectively guide the design and selection of the system. Thirdly, this paper combines the advantages of normal vector features and *FPFH* features in order to obtain local high-quality point pairs. In this paper, the bidirectional nearest neighbor distance criterion is adopted to screen the initial point pairs, and then the transformation matrix can be solved by unit quaternion method. After that, the precision registration is carried out by ICP. Finally, this paper conducts registration experiments on different algorithms. Experimental results show that the efficiency and accuracy of the improved algorithm are improved obviously. The accurate pose measurement method of curved surface parts and relevant experiment system studied in this paper can provide good references for the automatic grinding by robots.

Statements and Declarations

The authors declare that there are no conflicts of interest related to this article.

References

[1] LIU S, GE W M. Research on intelligent grinding tra-

jectory of industrial robot based on particle swarm optimization[J]. Journal of Tianjin University of Technology, 2020, 36(06)：8-12. (in Chinese)

[2] KONG X X. Identifying geomorphological changes of coastal cliffs through point cloud registration from UAV images[J]. Remote sensing, 2021, 13(16)：3152.

[3] SHU Z C, CAO S X, JIANG Q, et al. Pairwise registration algorithm for large-scale planar point cloud used in flatness measurement[J]. Sensors, 2021, 21(14)：4860.

[4] GUO Y, XIA Y H, YANG X Y, et al. A comparative study of large karst cave point cloud registration in various scanning modes[J]. Survey review, 2020, 52(374)：383-393.

[5] TSAI C Y, HUANG C H. Indoor scene point cloud registration algorithm based on RGB-d camera calibration[J]. Sensors, 2017, 17(8)：1874.

[6] MOHAMMAD K, KHALIL K, HOSSION A. Employing Nelder-Mead and gravitational search algorithm methods in point clouds registration process[J]. Procedia technology, 2015, 19：112-119.

[7] SHI G G, GAO X G, DANG X H. Improved ICP point cloud registration based on KD-tree[J]. International journal of earth sciences and engineering, 2016, 9(5)：2195-2199.

[8] SUN J H, ZHANG J, ZHANG G J. An automatic 3D point cloud registration method based on regional curvature maps[J]. Image and vision computing, 2016, 56：49-58.

[9] ZHANG X T, YANG B, LI Y H, et al. A method of partially overlapping point clouds registration based on differential evolution algorithm[J]. PLOS one, 2019, 13(12)：e0209227.

[10] LI L, CAO X Y, SUN J. Three-dimensional point cloud registration based on normal vector angle[J]. Springer india, 2019, 47(4)：585-593.

[11] RAN Y Y, XU X B. Point cloud registration method based on sift and geometry feature[J]. Optik, 2020, 203：163902.

[12] REN S Y, CHEN X D, CAI H H, et al. Color point cloud registration algorithm based on hue[J]. Applied sciences, 2021, 11(12)：5431.